JASA EXPRESS LETTERS ARTICLE asa.scitation.org/journal/jel

Depth-dependence of the underwater noise emission from melting glacier ice

Hari Vishnu,[1,a)] Grant B. Deane,[2] Oskar Glowacki,[3] Mandar Chitre,[1] Hayden Johnson,[2] Mateusz Moskalik,[3] and Dale Stokes[2]

[1]Acoustic Research Laboratory, 12A Kent Ridge Road, National University of Singapore, Singapore 119222
[2]Scripps Institution of Oceanography, University of California, San Diego, La Jolla, California 92093-0206, USA
[3]Institute of Geophysics, Polish Academy of Sciences, Warsaw, Poland

harivishnu@gmail.com, gdeane@ucsd.edu, oglowacki@igf.edu.pl, mandar@nus.edu.sg, h3johnso@ucsd.edu, mmosk@igf.edu.pl, dstokes@ucsd.edu

Abstract: Submarine-melting of ice at the glacier-ocean interface accounts for a large portion of the ice-loss at tidewater glaciers and produces sound via bubble-release. The sound production is dominant in the sub-surface region near the glacier-ocean interface. This depth-dependence of the sound is studied by melting ice blocks in a glacial bay at various depths up to 20 m and recording their acoustics over a large frequency range. The acoustic energy decreases with depth in line with expectations from the physics of the phenomenon and is fit to an exponentially decaying curve. The estimated variation will be useful for interpreting the sound in marine-terminating glaciers bays in terms of the submarine-melting activity.

[Editor: David R. Barclay] https://doi.org/10.1121/10.0017348

Received: 2 December 2022 **Accepted:** 30 January 2023 **Published Online:** 23 February 2023

1. Introduction

A significant component (60%) of the global sea level rise between 2006 and 2015 is attributed to melting of glaciers and ice-sheets (Oppenheimer *et al.*, 2019). At tidewater glaciers, a large fraction of the ice-loss is due to submarine glacier melting (SGM) at the glacier-ocean interface (GOI) (Motyka *et al.*, 2003; Wagner *et al.*, 2019). Hence, studying this phenomenon plays a key part in understanding glacial ice-loss. The SGM also undercuts glacier termini and consequently drives further ice-loss via calving [i.e., the mechanical loss of ice at GOI (Benn *et al.*, 2007)], which forms the other significant part of the freshwater flux (Motyka *et al.*, 2003; Wagner *et al.*, 2019).

Recently, a considerable amount of research has been undertaken on the acoustics in the Arctic, e.g., Collins *et al.* (2019), Dziak *et al.* (2015), and Pettit *et al.* (2012), including at tidewater glaciers which are shown to be highly noisy environments with time-varying acoustic levels (Deane *et al.*, 2019; Deane *et al.*, 2014; Pettit *et al.*, 2015) and often complicated propagation characteristics in the acoustic channel (Glowacki *et al.*, 2016; Zeh *et al.*, 2020). Calving and SGM both emit sound into the environment, and the acoustic signatures of these two ice-loss mechanisms are distinct. Thus, passive acoustic monitoring is a promising technique to monitor these ice-loss processes in Arctic regions (Schulz *et al.*, 2008). The acoustics of calving has been characterized well enough to the point where it can be used to quantify calving fluxes via acoustic monitoring (Glowacki and Deane, 2020). Here, we focus on the other ice-loss phenomenon, SGM, which generates impulsive sound due to the release of bubbles in glacier ice (Urick, 1971) that are pressurized as a result of the overburden pressure of the ice (Gow, 1968). Though it has been studied in previous works (Deane *et al.*, 2014; Glowacki *et al.*, 2018; Vishnu *et al.*, 2020), the acoustics of SGM still remains to be fully understood. To monitor SGM via passive acoustics, we first need to unravel the features and complexities of the SGM-induced acoustic field.

A noticeable feature of the SGM-induced acoustic field in glacial bays is its strong vertical directionality (Deane and Glowacki, 2018; Johnson *et al.*, 2020; Vishnu *et al.*, 2020). At the GOI, the sound is found to be strongest near the surface. Previous experimental studies have also indicated that the sound generated by bubble-release decreases with increasing depth below the surface (Deane and Glowacki, 2018). In order to quantify the decrease in energy with depth, we undertook a field experiment in a glacial bay whereby blocks of glacial ice were melted at different depths, and their acoustic signatures recorded. In this work, the aforementioned data is analyzed and an estimate of the sound level's depth-dependence is obtained, which is a crucial component for understanding the acoustic field. Furthermore, we show that the overall sound level's dependence on depth, frequency and temperature can be approximately decoupled.

[a)]Author to whom correspondence should be addressed.

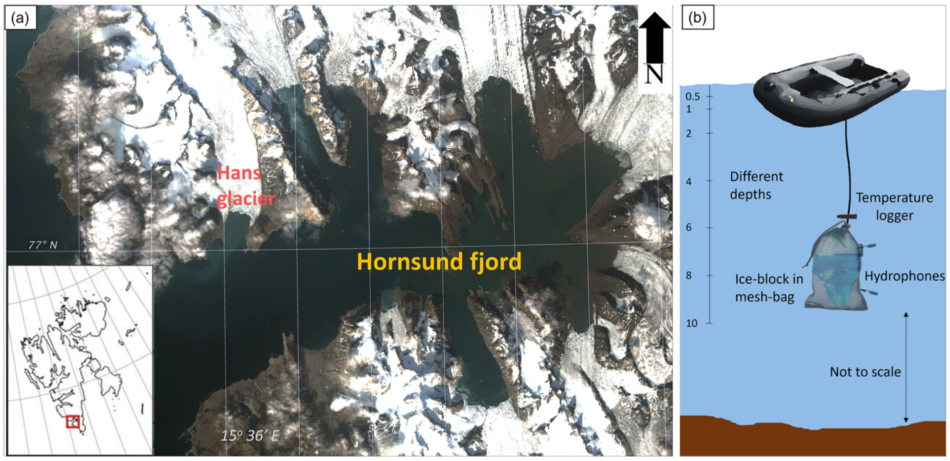

Fig. 1. (a) Location in Hornsund fjord where data were collected in the bay of Hans glacier. The fjord location is marked in red on the map of Svalbard shown in the inset image. (b) Illustration of field setup for acoustic measurements. The ice blocks were melted and their sound recorded far away from the glacier terminus, thus minimizing the impact of sound from the terminus on the measurements collected.

2. Experiment details and study region

The experiment was conducted in the Isbjornhamna bay in Hornsund fjord, whose location is shown in Fig. 1(a). With a positive mean annual trend in temperature of 1.14 °C per decade in the last four decades, this region has been warming six times faster than the global average (Wawrzyniak and Osuch, 2020), making it a model location to study incipient climate-change effects. Several studies have been undertaken on the acoustics in the glacial bays of this region (Deane and Glowacki, 2018; Deane *et al.*, 2014; Glowacki *et al.*, 2018). The region near the glacier terminus poses significant hazards for direct measurements due to the frequent sub-aerial and submarine calving events (Glowacki and Deane, 2020). Since the terminus region is difficult to access, this study utilizes blocks of ice which had recently calved from the terminus and studies their acoustic behaviour as a proxy for the behaviour of the terminus. Five such blocks of ice were collected in the bay of Hans glacier and cut into roughly cuboidal shape. These were packed into a mesh bag, taken to the bay in a boat, and dipped into the water on a line. The bag was lowered to different depths to observe the difference in melt sound with depth. The bag was expected to not influence the acoustics of the melting ice significantly, as its mesh size was large enough to let the bubbles be released freely. A temperature logger was mounted above the bag to measure the water temperature. The underwater sound of the melting was recorded using two High Tech Inc. 96-MIN hydrophones (High-Tech Inc, 2022) attached to the top and bottom of the bag [illustrated in Fig. 1(b)] and located 1.1 m away from the bag. Audio data were captured at a sampling rate of 96 kHz. Melting at depths of 0.5, 1, 2, 4, 6, 8, 10, 15, and 20 m were considered, although all the blocks were not necessarily melted at all of these depths. In Table 1 we tabulate the depths at which the blocks were melted, their weight before melting, the range of water temperatures recorded for each trial, and the average recording duration per depth for each block. The melting depths considered for all blocks result in 59 sound recordings for the analysis.

3. Analysis of recorded sound

3.1 Factors considered

The overall sound level due to melting depends on the depth of the ice, the temperature of the surrounding water region, and the properties of the ice. The temperature-dependence arises partly because of the fact that a higher temperature leads

Table 1. Measurements for each block suspended and recorded, including the melting depths, weight of the block before melting, range of water temperatures recorded at each melting depth, and average recording duration per depth for each block.

Block Number	Depths (in m below surface)	Starting weight (kg)	Range of water temperatures (°C)	Average recording duration per block (min)
1	2, 4, 6, 8, 10, 15, 20	4.36	2.3–4.5	2.6
2	2, 4, 6, 8, 10, 15, 20, 15, 10, 8, 6, 4, 2	3.83	2.3–3.6	2.4
3	2, 4, 6, 8, 10, 15, 20, 15, 10, 8, 6, 4, 2	6.43	2.4–4.3	2.1
4	2, 4, 6, 8, 10, 8, 6, 4, 2, 1, 0.5	4.22	2.5–4.3	2.1
5	2, 4, 6, 8, 10, 15, 20, 15, 10, 8, 6, 4, 2, 1, 0.5	5.16	2.7–4.0	2.3

to faster melting of the ice, in turn leading to an increase in the rate of impulsive events due to bubble-release. However, there could be additional reasons for the temperature-dependence. A hypothesized reason for the depth-dependence based on the physics of bubble-release from ice is as follows. For a bubble newly released from the ice, the energy available to generate sound scales with the difference between the bubble's internal gas pressure and hydrostatic pressure, apart from other factors (Deane and Glowacki, 2018). If the pressure differential decreases with depth (because hydrostatic pressure increases linearly with depth while the internal gas pressure does not increase as steeply), it would explain the observed decrease in acoustic energy of bubble-releases with depth. This depth-dependence can have a significant effect on the net SGM-induced acoustic field observed in the bay and thus warrants a deeper examination. Furthermore, it is not clear whether these dependencies of sound level on depth and temperature vary across the different frequencies in the spectrum of the signal (or, conversely, whether the spectral shape of melt sound depends on the depth and temperature). In order to answer these questions, we analyze the sound level in terms of three factors: the depth, frequency, and water-temperature.

3.2 Preprocessing

The timeseries due to the melting exhibits impulses due to the explosion of bubbles from the ice, as shown in Fig. 2, which make up a significant portion of the acoustic energy in the recording (Urick, 1971). These temporally concentrated impulses tend to stand out from the background noise, which is more temporally spread out. In order to isolate out the melt-induced acoustic events from the background noise, we first bandpass filter the recorded timeseries within the 0.5–20 kHz band, within which the melt sound was dominant. An example of a such a timeseries is shown in Fig. 2(a). The melt acoustic events are then identified as the outliers [red in Fig. 2(a)] that stand apart from the background noise envelope, using a thresholding-based approach. Melt-induced events are identified as the instants where the magnitude of at least 0.1 ms of continuous data exceeds the threshold.

For further analysis, we only consider acoustic events in the timeseries at least 10 s after the block is lowered into the water, to give the ice time to equilibrate to the local water conditions. The equilibration time is decided for each block based on observation of the envelope of the acoustic timeseries. The amplitudes of detected bubble-release events are normalized to a reference distance of 1 m from the ice block. We analyze the data in terms of the energy spectral density (ESD) of the melt signal sound pulses. The ESD for each block of data corresponding to an event is computed in units of J/Hz by first computing the power spectral density of the data using 128 fast-Fourier transform points, and multiplying it by the event duration and the factor $4\pi/(\rho c)$. The ESD of the background noise is then subtracted from the ESD of the data, which yields the total energy in the melt signal pulse. The average ESD of the events for each block is computed and represented as a function $P(f, y, T)$ of frequency f, depth y at which the block is melted, and water-temperature T recorded during the melting. The ESD is converted to decibels as $P_d(f, d, T) = 10\log_{10}(P(f, y, T)/P_0)$, where P_0 is a reference of 1 J/Hz. This yields ESD estimates from the data tabulated across 59 temperature values (one measurement for each depth at which each block was melted) and 9 depth points as described earlier.

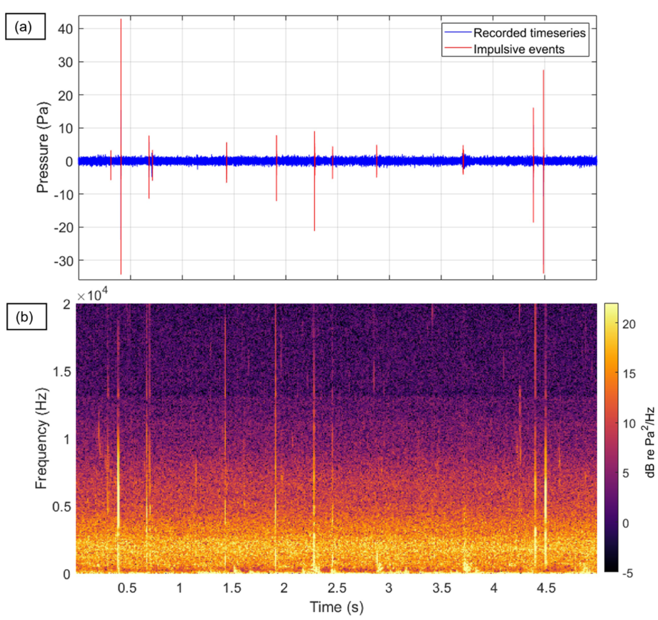

Fig. 2. (a) A sample 5-s long recorded timeseries (blue) and the impulsive events identified in this timeseries (red), and (b) spectrogram of this timeseries showing the broadband nature of the impulses.

3.3 Dependence of the ESD on frequency, depth, and temperature

We undertake a multi-linear polynomial regression (MLPR) (Seber and Lee, 2003) of $P_d(f, d, T)$ to analyze the dependence of the ESD on frequency, depth, and water temperature. In order to account for possible nonlinear variations in the dependence and coupling between the variables, we model the ESD as having a quadratic dependance on frequency, depth, water temperature and their second-order combinations, which are the factors in the tested hypothesis. Justification for a polynomial regression comes from the Weierstrass approximation theorem, which states that any continuous function on a finite interval can be approximated arbitrarily closely by a polynomial (Seber and Lee, 2003). We also include second-order "cross-terms" in the model as factors to test whether the ESD depends on interactions between these terms, or whether the dependences on each of these terms can be separated. We emphasize that the motivation of this exercise is not to fit an exact model to the variation of ESD as a function of these parameters, but rather to gauge whether there is a significant dependence on them in the first place, and the extent of cross term coupling. The MLPR model is expressed as

$$P_d(f, y, T) = c_1 f + c_{1,1} f^2 + c_2 y + c_{2,2} y^2 + c_3 T + c_{3,3} T^2 + c_4 + c_{1,2} f \times y + c_{1,3} f \times T + c_{2,3} y \times T, \quad (1)$$

where the constants c_1 through c_4 and $c_{1,1}$, $c_{2,2}$, $c_{3,3}$, $c_{1,2}$, $c_{1,3}$, and $c_{2,3}$ are determined by the model fit. MLPR statistics with the quadratic model in Eq. (1) are summarized in Table 2. It shows the p-values for each factor, which denote the false-alarm probability—the probability that the dependence observed on each factor may have resulted as an outcome of noise in the dataset. Thus, a smaller p-value indicates stronger evidence of a dependence on the corresponding factor. It can be seen that there is significant dependence of the spectrum on the depth and temperature with p-values all less than 0.01. For the depth and temperature ranges measured, the average ESD per event indicates an increasing trend with increase in temperature. The mechanisms underlying the temperature dependence are unknown at this time and worth exploring in future studies. For the focus of the current study, what is noticeably important is that the interaction terms between frequency, depth, and temperature are not significant at a threshold significance level of 0.01. Coupling between temperature and depth cannot be discarded at the 0.05 level but is not considered further here. At the 0.01 level of significance, the energy spectrum can be expressed as a product of three terms as

$$P(f, y, T) = \alpha(y) \nu(T) \beta(f), \quad (2)$$

where $\alpha(y)$ indicates the depth-dependence, $\nu(T)$ the temperature-dependance of the spectrum, and $\beta(f)$ indicates the spectral shape of acoustic bubble release events. The result in Eq. (2) is an important one, because it allows us to treat the effect of the spectral shape, depth, and temperature independently. Having established this and shown that there is a statistically significant dependence of the acoustic energy on the depth, we are now in a better position to estimate the average depth-dependence $\alpha(y)$.

3.4 Estimation of depth-dependence

Since variation of the source level with frequency, water-temperature and depth are empirically shown to be somewhat independent, we can now treat the depth-dependence separately from other dependencies. We focus on the frequency band of 1–3 kHz, since this is the band with highest signal-to-noise ratio of melt sound (Pettit *et al.*, 2015). We integrate the source energy spectra across this melt frequency-band to obtain the total frequency-integrated sound energy for each run as

$$E(y, T) = \int_{1000}^{3000} P(f, y, T) df. \quad (3)$$

To estimate the average $\alpha(y)$, the energy-depth variation for each run is first normalized to its value at 2 m to account for the variation in internal pressures and thus acoustic levels across different blocks. In this work, since we are focusing only on the *trend* of variation in acoustic energy with depth, and not the absolute level of the energy, it is necessary to normalize the energy-depth dependence for each run. The value at 2 m is chosen for normalization as we have the most number of data points at this depth. Finally, we estimate $\alpha(y)$ as the weighted average of the normalized variation for all the blocks, with the weight equal to the number of detected events at each depth for each block. The weighted-average normalized depth-dependence variation is plotted in Fig. 3 (red circles). It shows that the average acoustic energy decreases with an increase in the melting depth. This agrees with our understanding that the acoustic energy of bubble release events depends on the difference between the bubble's internal gas pressure and the hydrostatic pressure (Deane and Glowacki, 2018; Johnson *et al.*, 2021). At the surface, there is sufficient pressure difference to cause energetic bubble release events,

Table 2. Multi-linear regression of the dependence of melt spectrum on frequency f, depth y, and temperature T.

Controlling factor	f	f^2	y	y^2	T	T^2	$f \times y$	$f \times T$	$y \times T$
P-value	0.11	0.0017	0.0078	0.0015	6×10^{-5}	2×10^{-5}	0.88	0.30	0.044

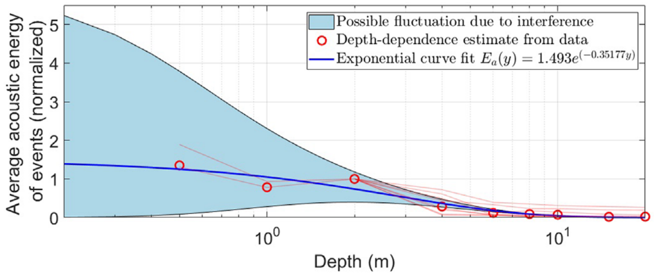

Fig. 3. Depth-dependence of the average acoustic energy of bubble-release events, estimated from the data via averaging (normalized to the value at 2 m depth) and fit to an exponentially decaying curve (blue). The red lines show estimates from each melting run of the blocks normalized to their value at 2 m depth. The light blue zone shows the possible range of fluctuation in the measured signal from the exponential curve fit, due to interference of the direct path with the surface-reflected path.

but as the depth increases, the hydrostatic pressure increases linearly whereas the internal pressure does not increase as steeply as the hydrostatic pressure, leading to a fall in acoustic energy. Below a certain cutoff depth, the pressure difference is expected to be small and hence the acoustic energy may be negligible.

We now fit, to the estimated data-based depth-dependence, an exponentially decaying curve defined as

$$E_a(y) = m_1 e^{(m_{(2)} y)}, \tag{4}$$

where m_1 and m_2 are free variables to be estimated. The fitting is done using MATLAB, and the curve thus obtained is shown in Fig. 3 (blue curve). The curve fit suggests that at a depth of 13.1 m, the average acoustic level is expected to fall below 1% of that at the surface, which is roughly consistent with observations in our previous work (Vishnu *et al.*, 2020). Note that while the estimated mean acoustic energy (red circles) shows a monotonic increase with decreasing depth, two of the data points exhibit a deviation from this trend. This deviation in the data may be because at shallow depths, the direct and surface-reflected acoustic paths from the sound source due to bubble release interfere to a significant degree. At large depths, the surface-reflected energy constitutes too small a fraction of the direct path energy to cause any serious interference—for example, at a depth of 4 m, the surface-path contains only 1.8% the energy of the direct path. However, at a shallow depth of 0.5 m, the surface-reflected path contains 55% the energy of the direct path, which could lead to noticeable interference effects. The range of fluctuation from the exponential curve possible in the measured sound due to interference effects is shown in Fig. 3, under the assumption that the sea-surface is perfectly reflective. It can be seen that non-monotonic deviation of the data line from the mean curve at shallow depths lies within this range.

4. Concluding remarks

The depth-dependence of the sound level due to submarine-melting of glacier ice has a significant effect on the acoustic field in the glacial bay. This depth-dependence is investigated via an experiment in a glacial bay in Hornsund fjord, Svalbard, in which ice blocks were melted at different depths. The analysis shows that the acoustic level due to ice-block melting exhibits a significant dependence on the depth and water-temperature. At the 0.01 significance level, the dependence of the acoustic spectrum on frequency, depth, and temperature can be decoupled, providing analytical apparatus that could be helpful in modeling the acoustic field's spatial variation in the bay. The coupling cannot be neglected at the 0.05 level, and this warrants further investigation which will be undertaken in the future. The estimated depth-dependence indicates that in the study region, the sound level due to melting ice-blocks falls to negligible levels by a depth of 13.1 m. More detailed measurements are needed to verify how this compares with the mean depth of the acoustically active zone of melting ice at the GOI, which may be different from the figure estimated here due to several possible reasons, listed below:

(1) Unlike the ice-blocks used in this study, the ice at the glacier may experience an increase in mean pressure with increasing depth below the glacier surface as indicated in studies in other regions (Gow, 1968). This could lead to the energy-depth variation at the GOI being different from that estimated here.
(2) Even at similar depths at the same glacier, there could be a significant variability in bubble internal pressures horizontally across the glacier face. Additionally, the presence of subglacial meltwater discharge outlets at some spots along the glacier face may increase the melting by up to an order of magnitude (Wagner *et al.*, 2019). These may further modulate the acoustically active zone and lead to fluctuations, which we do not capture in our study.
(3) It is not known to us what depth at the glacier terminus is represented by the ice-blocks used in our study. In a previous study, submarine calving events at Hansbreen were estimated to be at least 8–10 times less frequent than sub-aerial calving events (Glowacki, 2022). Warren *et al.* (1995) estimated that submarine events accounted for about 27% of the total calving flux and 7% of the calving events at Glaciar San Rafael in Chile. Thus, if most of the ice-blocks considered here resulted from sub-aerial calving at the terminus, they originated from a point on the glacier above the water surface.

Hence, their internal pressure may be low compared to ice at deeper regions of the glacier. If this aspect is accounted for, and overburden pressure does play a significant part in affecting the acoustics at the glacier, it is likely that the mean acoustically active depth at the GOI may be higher than the figure estimated here for the ice-blocks. Conversely, the acoustically active depth at the GOI may be lower than that estimated here if the blocks had resulted from submarine calving from a deeper point on the GOI than considered here.

(4) At different glaciers, the different properties of ice may further modulate the active zone.

Thus, direct acoustic measurements at the GOI are the only way to fully and conclusively understand the depth-dependence of acoustic activity there. Furthermore, note that the scope of the MLPR analysis on acoustic activity undertaken here is limited to dependencies of the types shown in Eq. (1), namely, the first and second order polynomial terms of the factors. However, it may not cover other nonlinear functional dependencies and coupling terms between the factors. Notwithstanding these limitations, the acoustically active depth estimated in this work gives a first-cut understanding of the acoustic activity of the submarine-melting process transpiring at the GOI and its depth-dependence. This is a valuable first step towards studying the acoustic activity at the GOI given the difficulty in directly studying it. These will form an important part of model-based interpretation of the spatial variation of the acoustic field in glacial bays in terms of the melt activity (Vishnu *et al.*, 2021). In the future, this can aid our efforts towards estimating the submarine melt-rates at marine-terminating glaciers, which is a crucial piece of information for modelling climate-change impacts.

Acknowledgments

This work was possible due to the support of grants from the National Research Foundation, Prime Minister's Office, Singapore under its Marine Science Research and Development Program MSRDP P-42, U.S. Office of Naval research Grant No. ONR-N00014-17-1-2633, National Science Foundation Grant No. OPP-1748265, the Institute of Geophysics, Polish Academy of Sciences Grant No. 2a/IGF PAN/2017, and statutory activities No. 3841/E-41/S/2019 of the Ministry of Science and Higher Education of Poland. We thank Christian Powell for his help in collecting the data. We also thank the staff at the Polish Polar Station, Hornsund, for all the support they have provided, and for maintaining the oceanographical monitoring with conductivity-temperature-depth profiles.

References and links

Benn, D. I., Warren, C. R., and Mottram, R. H. (**2007**). "Calving processes and the dynamics of calving glaciers," Earth-Sci. Rev. **82**(3-4), 143–179.

Collins, M. D., Turgut, A., Menis, R., and Schindall, J. A. (**2019**). "Acoustic recordings and modeling under seasonally varying sea ice," Sci. Rep. **9**(1), 1–11.

Deane, G. B., and Glowacki, O. (**2018**). "The vertical directionality of melt noise from a glacier terminus," J. Acoust. Soc. Am. **143**(3), 1833.

Deane, G. B., Glowacki, O., Stokes, M. D., and Pettit, E. C. (**2019**). "The underwater sounds of glaciers," Acoust. Today **15**(4), 12.

Deane, G. B., Glowacki, O., Tegowski, J., Moskalik, M., and Blondel, P. (**2014**). "Directionality of the ambient noise field in an Arctic, glacial bay," J. Acoust. Soc. Am. **136**(5), EL350–EL356.

Dziak, R. P., Bohnenstiehl, D. W. R., Stafford, K. M., Matsumoto, H., Park, M., Lee, W. S., Fowler, M. J., Lau, T. K., Haxel, J. H., and Mellinger, D. K. (**2015**). "Sources and levels of ambient ocean sound near the Antarctic Peninsula," PLoS One **10**(4), e0123425.

Glowacki, O. (**2022**). "Distinguishing subaerial and submarine calving with underwater noise," J. Glaciol. **68**(272), 1185–1196.

Glowacki, O., and Deane, G. B. (**2020**). "Quantifying iceberg calving fluxes with underwater noise," Cryosphere **14**(3), 1025–1042.

Glowacki, O., Deane, G. B., and Moskalik, M. (**2018**). "The intensity, directionality, and statistics of underwater noise from melting icebergs," Geophys. Res. Lett. **45**(9), 4105–4113, https://doi.org/10.1029/2018GL077632.

Glowacki, O., Moskalik, M., and Deane, G. B. (**2016**). "The impact of glacier meltwater on the underwater noise field in a glacial bay," J. Geophys. Res. Oceans **121**(12), 8455–8470, https://doi.org/10.1002/2016JC012355.

Gow, A. J. (**1968**). "Bubbles and bubble pressures in antarctic glacier ice," J. Glaciol. **7**(50), 167–182.

High-Tech Inc. (**2022**). "HTI-96-Min" http://www.hightechincusa.com/products/hydrophones/hti96min.html (Last viewed February 14, 2023).

Johnson, H. A., Deane, G. B., Stokes, M. D., Glowacki, O., Moskalik, M., Chitre, M., and Vishnu, H. (**2021**). "Predicting the acoustic energy radiated by melting glacier ice," J. Acoust. Soc. Am. **150**(4), A329.

Johnson, H. A., Vishnu, H., Deane, G. B., Tuckman, P., Glowacki, O., and Moskalik, M. (**2020**). "Depth dependence of acoustic signals produced by bubble release events in melting glacier ice," J. Acoust. Soc. Am. **148**(4), 2483.

Motyka, R. J., Hunter, L., Echelmeyer, K. A., and Connor, C. (**2003**). "Submarine melting at the terminus of a temperate tidewater glacier, LeConte Glacier, Alaska, U.S.A.," Ann. Glaciol. **36**, 57–65.

Oppenheimer, M., Glavovic, B., Hinkel, J., van de Wal, R., Magnan, A., Abd-Elgawad, A., Cai, R., Cifuentes-Jara, M., DeConto, R., Ghosh, T., Hay, J., Isla, F., Marzeion, B., Meyssignac, B., and Sebesvari, Z. (**2019**). "Sea level rise and implications for low-lying islands, coasts and communities," in *IPCC Special Report on the Ocean and Cryosphere in a Changing Climate*, edited by H.-O. Portner, D. Roberts, V. Masson-Delmotte, P. Zhai, M. Tignor, E. Poloczanska, K. Mintenbeck, A. Alegria, M. Nicolai, A. Okem, J. Petzold, B. Rama, and N. M. Weyer.

Pettit, E., Lee, K. M., Brann, J. P., Nystuen, J. A., Wilson, P. S., and Neel, S. O. (**2015**). "Unusually loud ambient noise in tidewater glacier fjords: A signal of ice melt," Geophys. Res. Lett. **42**, 2309–2316, https://doi.org/10.1002/2014GL062950.

Pettit, E., Nystuen, J., and O'Neel, S. (**2012**). "Listening to glaciers: Passive hydroacoustics near marine-terminating glaciers," Oceanography **25**(3), 104–105.

Schulz, M., Berger, W. H., and Jansen, E. (**2008**). "Listening to glaciers," Nat. Geosci. **1**(7), 408–408.

Seber, G., and Lee, A. (**2003**). *Linear Regression Analysis*, 2nd ed. (Wiley, New York).

Urick, R. J. (**1971**). "The noise of melting icebergs," J. Acoust. Soc. Am. **50**(1B), 337–341.

Vishnu, H., Deane, G. B., Chitre, M., Glowacki, O., Stokes, D., and Moskalik, M. (**2020**). "Vertical directionality and spatial coherence of the sound field in glacial bays in Hornsund Fjord," J. Acoust. Soc. Am. **148**(6), 3849–3862.

Vishnu, H., Deane, G. B., Chitre, M., Glowacki, O., Stokes, M. D., Moskalik, M., and Johnson, H. A. (**2021**). "Spatial variation in acoustic field due to submarine melting in glacial bays," J. Acoust. Soc. Am. **150**(4), A327–A328.

Wagner, T. J., Straneo, F., Richards, C. G., Slater, D. A., Stevens, L. A., Das, S. B., and Singh, H. (**2019**). "Large spatial variations in the flux balance along the front of a Greenland tidewater glacier," Cryosphere **13**(3), 911–925.

Warren, C. R., Glasser, N. F., Harrison, S., Winchester, V., Kerr, A. R., and Rivera, A. (**1995**). "Characteristics of tide-water calving at glaciar San Rafael, Chile," J. Glaciol. **41**(138), 273–289.

Wawrzyniak, T., and Osuch, M. (**2020**). "A 40-year high arctic climatological dataset of the Polish polar station Hornsund (SW Spitsbergen, Svalbard)," Earth Syst. Sci. Data **12**(2), 805–815.

Zeh, M. C., Glowacki, O., Deane, G. B., Ballard, M. S., Pettit, E. C., and Wilson, P. S. (**2019**). "Model-data comparison of sound propagation in a glacierized fjord with a brash ice top surface," Proc. Mtgs. Acoust. **36**, 070005.